

# Impact-modified epoxy resin with glassy second component

SUNG C. KIM\*, HUGH R. BROWN

IBM Almaden Research Center, 650 Harry Road, San Jose, California 95120-6099, USA

A resorcinol-based epoxy resin was modified by incorporating a glassy second component. The mixture showed a heterogeneous morphology with two clearly defined phases, one phase rich in oligomer, the other phase composed mainly of resorcinol epoxy resin. The fracture toughness measured as  $G_{Ic}$  and  $K_{Ic}$  values showed an increase from  $174 \text{ J m}^{-2}$  and  $0.89 \text{ MN m}^{-1.5}$  in pure epoxy resin to  $431 \text{ J m}^{-2}$  and  $1.36 \text{ MN m}^{-1.5}$  in 30% oligomer modified resins. The scanning electron micrographs showed that the oligomer-rich phase exhibited ductile failure behaviour and formed the dispersed phase at low concentrations while it was the continuous matrix when the concentration was 30%. Optical observations on the failure mode of thin films of the oligomer-modified epoxy resin showed the existence of both inter-face failure and considerable distortion in both phase.

## 1. Introduction

The use of epoxy resin in high-performance structural materials has been increasing recently, particularly in applications for high-performance adhesives and advanced composite matrix materials in the aerospace and electronics industries. The combined mechanical properties of high modulus and high strength at relatively high temperatures make the material suitable for these applications. The major drawbacks of epoxy resin, however, are brittleness and high moisture absorption. There have been many studies on the modification of epoxy resin by the incorporation of a second component. The most common material used as the second component is the rubbery polymer poly (butadiene co-acrylonitrile) with reactive end groups of either carboxyl (CTBN) or amine functionality. These end groups react with the oxirane ring in the epoxy resin [1-9]. The fracture toughness of these materials is dependent on the toughness of the original epoxy and also the particle size, particle volume fraction, interfacial bonding and the properties of the rubbery component. The relative compatibility of the modifier in the epoxy as well as the rate of reaction determines the particle size and the interfacial bonding and also affects the particle volume fraction as phase intermixing often occurs. The mechanisms that have been proposed for energy absorption in these materials assume either that the failure energy is mainly dissipated in plastic deformation in the epoxy matrix which is itself initiated by voiding within the rubber particles [3-7] or, alternatively that the crack is bridged by the rubbery component and as the crack propagates the strain energy within these rubber fibrils is lost [8, 9]. There are problems in the latter approach particularly in terms of the use of fracture mechanics to describe the failure of such small rubber fibrils.

They are smaller than the energy dissipation volume in the customary macroscopic rubber fracture mechanics tests. In addition it is hard to see how sufficient energy can be dissipated in such a small volume of rubber.

The incorporation of a hard spherical filler such as aluminium trihydrate [18] or glass spheres also improves the fracture toughness of the resin to some degree. The energy absorbing mechanism for these materials is described as a crack-pinning process [10, 11]. The crack front travelling through the material is slowed when it encounters an inhomogeneity and the crack is considered to be pinned at that point. The pinned crack front is presumed to bow forward between the pinning points until semi-circular segments of the neighbouring bowed fronts overlap and the crack breaks away.

The incorporation of the glassy polymer component has also been reported. Both poly(aryl ether sulphone) [12] and phenolic hydroxyl terminated bisphenol-A polysulphone oligomers [13] have been used as the glassy component. The poly(aryl ether sulphone) was added originally for the purpose of increasing the viscosity during the hot lay-up process. The hydroxyl end groups of either polysulphone can react with the oxirane groups of the epoxy but the extent of reaction is considered to be higher with the phenolic hydroxyl terminated bisphenol-A polysulphone oligomer. The chemical structures of the polysulphones are very similar to the diglycidyl ether bisphenol-A (DGEBA) type epoxy resin cured with the diamino diphenyl sulphone (DDS) curing agent. Phase separation is noted as the reaction proceeds, but the domain sizes in these cases are quite small (in the range of  $0.1 \mu\text{m}$ ) due to the similarity in their chemical structure. (A similar phenomenon is well known with CTBN additions to epoxies where the very compatible high nitrile

\*Permanent address: Department of Chemical Engineering, Korea Advanced Institute of Science and Technology, P.O. Box 131, Cheongryang, Seoul, Korea.

CTBNs give small rubber phases [1, 2]. The polysulphone-rich phase forms the dispersed phase and some degree of enhancement in the fracture toughness is observed which was thought to be due to the ductile deformation of the dispersed phase [13].

The present paper describes the morphology and fracture toughness behaviour of an epoxy resin modified with a ductile glassy oligomer with reactive end groups. The morphology of the materials used in this study changes from a dispersed ductile phase in a brittle matrix to a brittle dispersed domain in a ductile glassy matrix with increased oligomer content.

## 2. Experimental techniques

### 2.1. Sample preparation

The epoxy used was Heloxy 69, a resorcinol-based material from Wilmington Chemical, that was cured with 44' diamino diphenyl sulphone (DDS). The glassy oligomer, of undisclosed composition, was obtained from Hercules Chemical. It had a glass transition temperature,  $T_g$ , of 168°C. Samples were prepared in a conventional manner and cured in a teflon mould at 185°C for 2 h and 210°C for 2 h before slowly cooling to room temperature at 1°C min<sup>-1</sup>. Thin films for optical observation were obtained by curing between two rock salt plates (either polished or cleaved surfaces). The films, whose thickness was in the range 10 to 40 µm were obtained after dissolving the rock salt plates in water. Results will be presented in unmodified epoxy and epoxy containing 10% and 30% modifier.

### 2.2. Measurement

#### 2.2.1. Fracture test

The fracture toughness measurements were done according to the ASTM E399-83 procedure. To create a crack tip, the specimen was kept in an oven at 210°C under nitrogen for 10 min and then a crack of 2.8 to 3.5 mm in length was made by pressing a razor blade on to the centre of the specimen. The sample was also cooled at 1°C min<sup>-1</sup> to room temperature after the cut was made and the specimen had been annealed for 10 min at 210°C. The crack length-to-width ratio was in the range of 0.22 to 0.30. Conventional three-point bending tests were conducted with span length of 50 mm and a crosshead speed of 1.25 mm min<sup>-1</sup>.

The Young's modulus was measured separately by three-point bending on specimens with dimensions of 63.5 mm × 12.5 mm × 3.2 mm. The span, length and the crosshead speed was the same as for the fracture toughness measurement.

#### 2.2.2. Scanning electron microscopy

The scanning electron micrographs were obtained on a Hitachi model S500 SEM on fracture surfaces sputter-coated with gold. The specimens were tilted towards the detector by about 20° to give the depth image in the micrograph.

#### 2.2.3. Thermal analysis

The glass transition behaviour was studied using the du Pont model 1090 Thermal Analyser along with model 982 DMA and model 910 DSC unit. The

TABLE I Glass transition temperature

Oligomer conc. (wt %)	$T_g$ , onset (°C)	$T_g$ , midpoint (°C)
0	162	172
10	163	173
30	155	166

specimen dimensions for the DMA analysis were 31.75 mm × 12.5 mm × 3.2 mm, the gap setting was 6.9 mm and the oscillation amplitude was 0.5 mm. The heating rates for both DMA and DSC runs were 5°C min<sup>-1</sup>.

### 2.2.4. Optical microscopy

The failure behaviour of the thin epoxy film was observed using the Jenoptic Jena AMPLIVAL polarizing microscope and the PERAVAL interphako unit. Thin films of 20 mm × 3 mm were stretched by a small tensile tester (PL-Minimat, Polymer Laboratories) placed on the microscope stage. A razor cut was made at the centre of the specimen and the crack tip sections were observed during the stretch using either phase contrast or crossed polars. The stretching was done manually to a stress level on the film of 22 to 23 MPa.

## 3. Results and discussions

### 3.1. Thermal and dynamic mechanical analysis

The glass transition temperatures of the oligomer-modified epoxy resins are listed in Table I and the DSC thermograms are shown in Fig. 1. Although the resin exhibits a two-phase morphology, the  $T_g$ s of the two phases are so close to each other that the thermogram does not show the individual  $T_g$ s. The incorporation of the oligomer slightly lowers the overall glass transition temperature of the modified resin.

The secondary transition temperature, which may be related to the ductility of the material, is shown by the DMA thermograms at subambient temperature. The pure epoxy resin shows transition at about

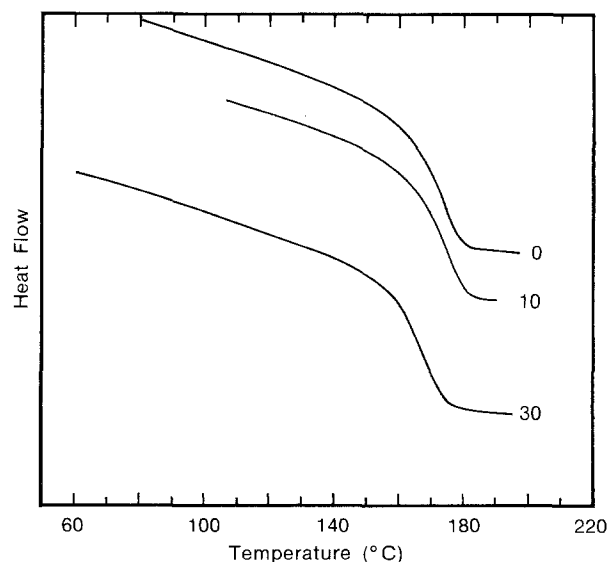


Figure 1 DSC thermograms of oligomer-modified epoxy resin.

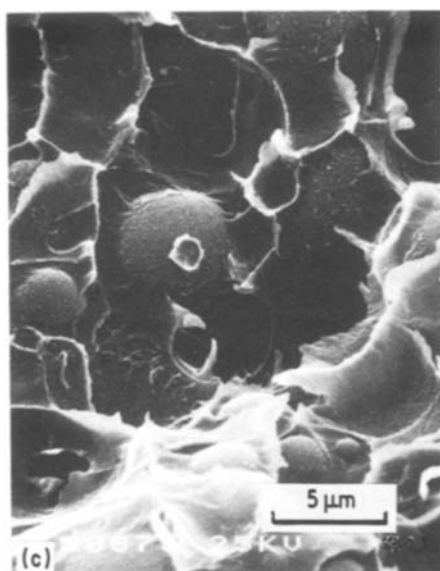
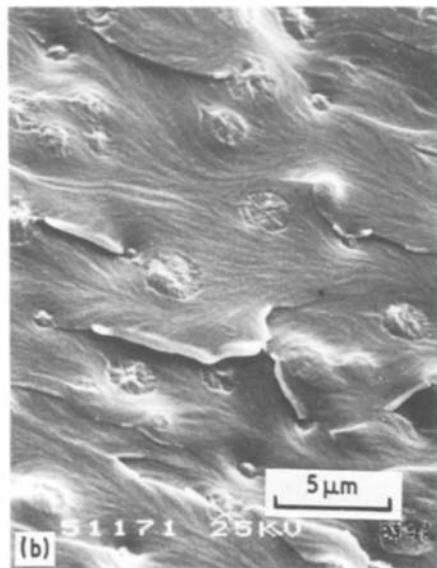
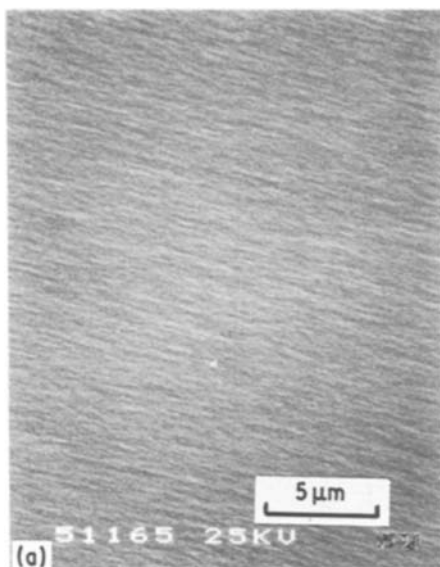


Figure 2 Scanning electron micrographs of the fractured surface of epoxy resin modified with: (a) 0%, (b) 10%, (c) 30% oligomer.

latter case was much smaller ( $0.1 \mu\text{m}$ ) because of the increased compatibility between the oligomer and the epoxy which had very similar chemical structures. In the 30% oligomer-modified epoxy resin, the average domain size of the dispersed phase, which is now composed of the hard spheres of the pure epoxy resin, is about  $4.3 \mu\text{m}$  (Fig. 3). The morphology of CTBN modified epoxies is thought to be controlled by a combination of kinetic and equilibrium parameters depending on the individual system and cure conditions and the same situation probably occurs here. For example it has been shown by light scattering during the cure process that in one system the phase

–  $28^\circ\text{C}$ . As the oligomer concentration is increased, the secondary transition is shifted towards lower temperature.

### 3.2. Morphology

The scanning electron micrographs of the fracture surfaces are shown in Fig. 2. A well-defined two-phase morphology is clearly shown in all the oligomer-modified samples. The oligomer-rich phase also shows considerable ductile deformation while the failure in the epoxy-rich phase is much more brittle. A phase inversion between oligomer-rich particles in an epoxy-rich matrix and epoxy-rich particles in an oligomer-rich phase occurs in compositions containing between 10% and 30% oligomer. Ductile deformation is evident in the matrix phase in 30% oligomer concentration while it is seen in the dispersed phase in 10% oligomer concentration.

The average dispersed domain size of the 10% oligomer modified epoxy resin is  $1.7 \mu\text{m}$ . Similar morphology was also observed in bisphenol-A type epoxy resins modified by 10 to 15% bisphenol-A polysulphone oligomer which has phenolic hydroxyl end groups to react with the epoxide [13]. The domain size in the

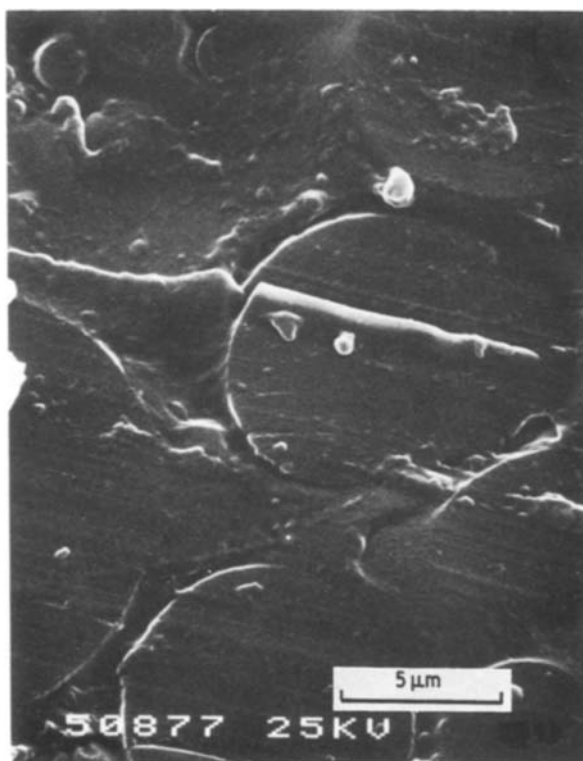


Figure 3 Scanning electron micrographs of the razor cut surface of epoxy resin showing dispersed domains, 30% oligomer.

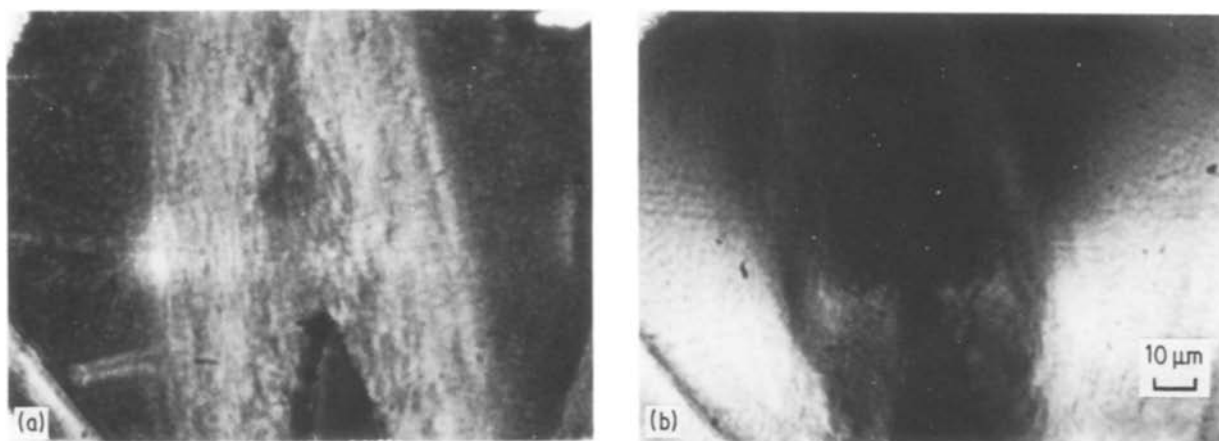


Figure 4 Optical micrographs of crack propagation through thin films of 30% oligomer-modified epoxy resin under 22.3 MPa stress ( $\times 520$ ). (a) Phase contrast, (b) cross polar.

separation occurs well before gelation and the light scattering pattern appears to grow only in intensity but not change in shape during the phase-separation process [14]. It would appear likely that in this case the morphology produced was an equilibrium one. However, in the majority of published work it has been assumed that kinetic effects are important in the control of the morphology induced by phase separation. A relatively simple kinetic model based on the Flory–Huggins theory to give the driving force for phase separation [15] has been successful in explaining experimental observations of the effect of initial rubber concentration and cure temperature on phase morphology [1, 2].

Phase inversion at around 20% oligomer similar to that observed here has previously been reported in a number of CTBN–epoxy systems [1, 2, 14] and is predicted from a Flory–Huggins treatment where a critical point at 28% rubber was found. It is at concentrations close to the critical point that phase separations will occur earliest during the curing process so, other things being equal, it is in these systems that the second phase has the longest time to grow and so will be the largest.

The fractured surface of the pure epoxy resin shows a stable brittle crack propagation typical of a well-cured epoxy [16], the crack arrest lines typical of slip-

stick propagation [17, 18] were not observed (Fig. 3). The 10% oligomer content material shows relatively little oligomer and excellent interfacial adhesion as the crack always propagated through the domains.

The failure behaviour of the composition having an oligomer-rich continuous phase (30%) was quite different in appearance. Here the matrix shows considerable ductility and experiences a typical ductile failure with no evidence of deformation or failure in the epoxy spheres. A large amount of interface failure is, however evident.

### 3.3. Crack propagation in thin films

The optical micrographs of the cracks propagating through thin films of 30% oligomer modified epoxy resins are shown in Figs 4 and 5. In this material, the domains are large and have a broad size distribution. Around the crack tip there is a region approximately  $60\ \mu\text{m}$  wide which shows bright in positive phase contrast and was multicoloured in cross polars. This deformation zone round the crack tip is, therefore, highly birefringent and so must contain oriented material. The phase contrast in this region did not depend upon the polarization of the incident light so cannot originate in the birefringence. This is evidence that void formation occurs along with the orientation in the deformation zone.

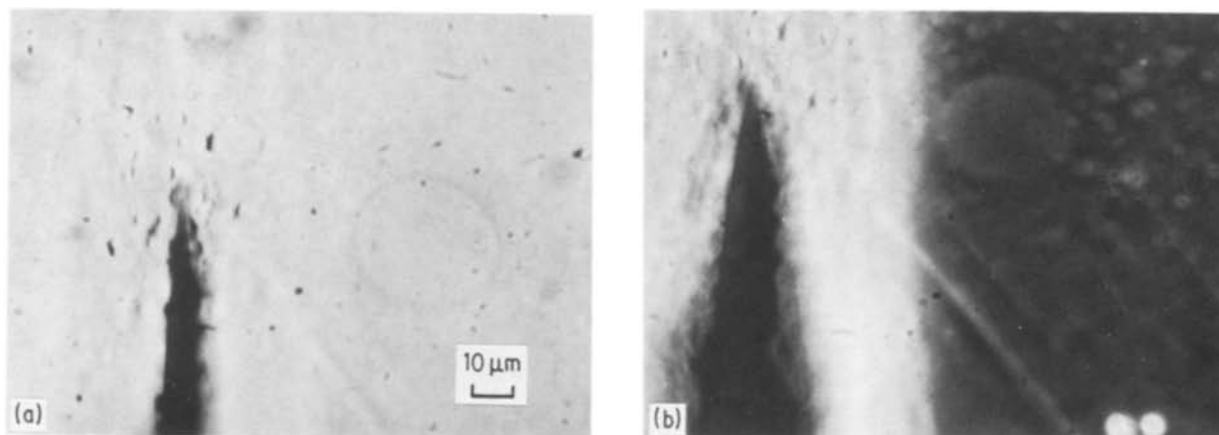


Figure 5 Optical micrographs showing dewetting in front of the crack tip advancing under 22.3 MPa stress in 30% oligomer-modified epoxy film ( $\times 520$ ). (a) Plain, (b) phase contrast.

TABLE II Effect of oligomer concentration on modulus and fracture toughness

Oligomer conc. (wt %)	$E$ (GPa)	$K_{Ic}$ ( $\text{MN m}^{-1.5}$ )	$G_{Ic}$ ( $\text{J m}^{-2}$ )
0	3.99	0.89	174
10	3.94	0.98	214
30	3.77	1.36	431

Around the crack tip dewetting and particle deformation are apparent. The dewetting, which is clear in a plain transmitted light optical micrograph, occurs around the poles of the particles that are close to the crack tip and hence in the region of maximum tensile stress. The particle deformation that is visible in these micrographs is not evident from the SEM fracture surface studies either because the spheres have by then relaxed or, more likely, because it is less easy to see the sphere deformation on the SEM pictures.

### 3.4. Fracture toughness and modulus

The fracture toughness and modulus results are listed in Table II. The modulus shows a gradual but relatively small decrease from 4.0 GPa in pure epoxy to 3.8 GPa in 30% oligomer-modified epoxy. Because the two phases are both glassy at room temperature, the morphological phase inversion is not evident in the modulus behaviour. The fracture toughness behaviour shows a gradual and monotonic increase as the oligomer concentration is increased. The change in fracture mechanisms from 0 to 10% oligomer concentration (change from homogeneous to heterogeneous morphology) and from 10% to 30% oligomer (phase inversion) is not reflected in any abrupt change in the fracture toughness behaviour.

The fracture energy,  $G_{Ic}$ , is similar to the  $K_{Ic}$  behaviour. The fracture energy increased from  $174 \text{ J m}^{-2}$  in pure epoxy to  $431 \text{ J m}^{-2}$  in 30% oligomer-modified epoxy. This is not as high as the rubber-modified epoxies [17] with  $G_{Ic}$  values of  $2000 \text{ J m}^{-2}$ , but is a respectable degree of toughening of a brittle epoxy, particularly as it is obtained without sacrificing the modulus and the high-temperature properties.

### 3.5. Fracture and toughening mechanisms

The main aim of this work was to gain information on the failure mode of epoxies that are toughened by the addition of a glassy second phase. It is worth considering initially whether any of the mechanisms that have been proposed to explain the toughening by rubbers might apply in this case. Kinloch *et al.* [3, 4] discussed in great detail in two recent publications the failure of both unmodified and rubber-modified epoxies as a function of temperature. They argued that in both materials the primary source of energy dissipation in failure was yielding and plastic shear flow in the matrix. The stress-whitening that occurred in the rubber-modified materials was interpreted as voiding in or around the rubber particles which was considered to be a secondary dissipation process. The role of the rubber particles was believed to be primarily one of causing stress concentrations which, particu-

larly if the particles cavitate, helps to initiate shear yielding in the matrix. They noted that the toughening extended down to the temperatures below the  $T_g$  of the rubber and suggested that there would still be an elastic stress concentration at these temperatures as the shear modulus of the rubber, which was just below  $T_g$ , would be significantly below that of the highly cross-linked matrix. This argument might apply to the materials examined here, though the  $T_g$  of the glassy modifier was  $\sim 160^\circ \text{C}$ , similar to that of the epoxy so the modulus difference can come only from the effect of cross-linking on modulus.

The other mechanism that has been proposed to explain rubber toughening is the crack-bridging model discussed in Section 1. In this model it is suggested that the energy dissipation occurs mainly in the rubber particles which are highly deformed when they bridge the crack. It is easy to imagine that a similar argument could be made in the case of glassy second-phase toughening so it is worth considering such an argument in more detail. The addition of 10% oligomer increased the toughness of the material from  $174$  to  $214 \text{ J m}^{-2}$  an increase of  $40 \text{ J m}^{-2}$ . The mean oligomer particle size in this material was  $2 \mu\text{m}$  so it is reasonable to assume that particles that would bridge the crack had their centres within  $0.5 \mu\text{m}$  of the crack plane. The total volume of oligomer per unit area of the crack that might form these bridges was  $10^{-7} \text{ m}^3$ . If a constrained yield stress of  $100 \text{ MPa}$  is assumed then the strain in the oligomer particles to absorb this energy would have been 400%. Fig. 3 shows clearly that no such strain occurred, in fact the strain in the oligomer particles was not very much greater than that in the matrix. It is clear from these considerations that the extra energy dissipation must either be in the particles some distance from the crack plane or in the matrix. It seems likely that the situation is similar to that in the rubber-toughened materials, the particles yield before the matrix and, as they are not greatly cross-linked and so do not strain harden, a stress concentration is caused in the epoxy which will initiate localized yielding between the particles.

The fracture surfaces look very different in the material with oligomer content of 30% from that observed on the 10% oligomer material. In the former the oligomer is the matrix and its ductility is reflected in much more evident ductile deformation on the fracture surface. It is significant that the toughness changes continuously through this phase inversion so this apparent large change in ductility does not have much effect on the fracture energy. The optical micrographs of cracks in thin films show that there was yield between the particles, fine scale voiding and also interface failure at the poles of the epoxy particles. The distortion of the epoxy spheres, which was evident in these micrographs, demonstrates clearly that considerable deformation can occur in epoxies near a crack tip. This deformation must be the main dissipation process in the lower oligomer content materials. The continuous change of the fracture toughness as a function of oligomer content together with the large change in local, fracture surface, ductility show that the depth of the ductile region probably decreases as

the oligomer content is increased through the phase inversion. This is not surprising as the ductile matrix material might be expected to show more strain softening and hence more strain localization than the epoxy matrix material.

#### 4. Conclusions

Epoxy resins can be toughened by the addition of a second phase of a glassy polymer. The degree of toughening is relatively modest compared with that obtainable with a CTBN-rubber second phase but the modulus and softening temperature are not significantly reduced by the modification. The microstructure of these materials is similar to that found in the rubber-toughened materials with a phase inversion between 10% and 30% modifier. For the low modifier contents the mechanism of toughening involves yielding of the modifier particles initiating local yield in the epoxy matrix. It is this yielding in the epoxy that is the main deformation process which dissipates the failure energy. For the higher modifier contents there is considerable deformation in the modifier matrix and a small amount of deformation in the epoxy particles. In this case interface failure is significant and the fracture surfaces look much more ductile though the failure energy is not greatly higher than that at the lower modifier contents.

#### Acknowledgements

The authors wish to thank Mr John Duran and Mr Richard Siemens for their help in scanning electron microscopy and thermal analysis.

#### References

1. L. T. MANZIONE, J. K. GILLHAM and C. A. McPHERSON, *J. Appl. Polym. Sci.* **26** (1981) 889.
2. *Idem, ibid.* **26** (1981) 907.
3. A. J. KINLOCH, S. J. SHAW, D. A. TOD and D. L. HUNSTON, *Polymer* **24** (1983) 1341.
4. A. J. KINLOCH, S. J. SHAW and D. L. HUNSTON, *ibid.* **24** (1983) 1355.
5. C. B. BUCKNALL and T. YOSHI, *Br. Polym. J.* **10** (1978) 53.
6. R. A. PEARSON and A. F. YEE, *Polym. Mater. Sci. Eng.* **49** (1983) 316.
7. J. R. BITNER, J. L. RUSHFORD, W. S. ROSE, D. L. HUNSTON and C. K. RIEW, *J. Adhesion* **13** (1982) 3.
8. S. KUNZ-DOUGLASS, P. W. R. BEAUMONT and M. F. ASHBY, *J. Mater. Sci.* **15** (1980) 1109.
9. S. C. KUNZ, J. A. SAYRE and R. A. ASSINK, *Polymer* **23** (1982) 897.
10. F. F. LANGE and K. C. RADFORD, *J. Mater. Sci.* **6** (1971) 1197.
11. S. K. BROWN, *Br. Polym. J.* **12** (1980) 24.
12. C. B. BUCKNALL and I. K. PARTRIDGE, *Polymer* **24** (1983) 639.
13. J. HEDRICK, I. YILGOR, G. L. WILKES and J. E. McGRATH, *Polym. Bull.* **13** (1985) 201.
14. S. VISCONTI and R. H. MARCHESSAULT, *Macromol.* **7** (1974) 913.
15. R. J. J. WILLIAMS, J. BORRAJO, H. E. ADABBO and A. J. ROJAS, *Polym. Mater. Sci. Eng.* **49** (1983) 432.
16. S. YAMINI and R. J. YOUNG, *J. Mater. Sci.* **13** (1979) 1609.
17. R. A. GLEDHILL, A. J. KINLOCK, S. YAMINI and R. J. YOUNG, *Polymer* **19** (1978) 574.
18. A. J. KINLOCH and R. J. YOUNG, "Fracture Behavior of Polymers" (Applied Science, London, 1983).

*Received 1 September*

*and accepted 12 November 1987*